COMPDYN 2019
7th ECCOMAS Thematic Conference on
Computational Methods in Structural Dynamics and Earthquake Engineering
M. Papadrakakis, M. Fragiadakis (eds.)
Crete, Greece, 24–26 June 2019

EXPERIMENTAL AND NUMERICAL EVALUATION OF CORING EFFECTS IN REINFORCED CONCRETE COLUMNS

Giuseppe Santarsiero[1], Angelo Masi[1], Andrea Digrisolo[1], Vincenzo Manfredi[1], Giuseppe Ventura[1], Domenico Nigro[1], Biagio Difina[1]

School of Engineering, University of Basilicata, viale dell'Ateneo Lucano, 10, Potenza, Italy

{giuseppe.santarsiero, angelo.masi, andrea.digrisolo, enzo.manfredi, giuseppe.ventura}@unibas.it;

Abstract

The knowledge of in-situ material properties is the first step in the assessment process of existing structures and, where needed, in the design of the consequent strengthening interventions. In order to achieve this goal, destructive (DT; e.g., cores) and non-destructive (NDT; e.g., ultrasonic, rebound) test methods are generally adopted, either alone or combined. Although many literature papers and guidelines propose to minimize the number of cores in the estimation of the concrete strength in reinforced concrete structures, the European and Italian codes prescribe that the estimation of in-situ strength has to be mainly based on cores drilled from the structure (DT). In this framework, the paper reports results of an experimental program aimed at evaluating the effects of core tests on RC columns, as well as the effectiveness of the structural restoration of drilling holes. Specifically, three sets of column specimens have been considered: (i) drilled columns, (ii) drilled and subsequently restored columns, and (iii) reference not drilled (as-built) columns. Compression tests have been carried out on each column and the results have been compared with the prediction based on codes or other literature approaches. This helped to recognize the main phenomena affecting the column members behavior under axial loads.
At the same time, the authors calibrated detailed finite element models based on the experimental results of the tests carried out on column specimens. An advanced Fem tool was used to set-up 3D models. Numerical simulations aimed at better understanding the failure mechanism, especially in the presence of the hole related to the core extraction. The role of longitudinal and transverse reinforcement has been evaluated, highlighting that concrete crushing in the areas around the hole causes the early buckling of rebars, leading to premature failure of drilled column specimens.

Keywords: Destructive tests, concrete strength, core drilling, finite element model, nonlinear numerical simulation.

1 INTRODUCTION

The investigation of structural characteristics (geometry, structural details, materials quality, etc.) is a crucial step in the assessment of existing reinforced concrete (RC) structures [1, 2] and, where needed, in the design of consequent strengthening interventions [3]. Specifically, the knowledge of in-situ material properties is the first step in the assessment process of existing structures. In order to achieve this goal, destructive (DT; e.g., cores) and non-destructive (NDT; e.g., ultrasonic, rebound) test methods are generally adopted, either alone or combined. Although many literature papers and guidelines propose to minimize the number of cores in the estimation of the concrete strength in reinforced concrete structures, the European and Italian codes prescribe that the estimation of in-situ strength has to be mainly based on cores drilled from the structure (destructive test, DT). Non-destructive tests (NDTs) can only supplement coring, thus permitting a more economical and representative determination of concrete properties throughout the whole structure under examination. In this framework, the paper reports results of an experimental program aimed at evaluating the effects of core tests on RC columns, as well as the effectiveness of the structural restoration of drilling holes. Twenty RC column specimens (dimension 30cm x 30cm x 80cm) have been purposely built and tested by both non-destructive and destructive tests. Specifically, after the preliminary campaign of ultrasonic tests performed on all structural members, three sets of column specimens have been considered: (i) drilled columns (3 specimens), (ii) drilled and subsequently restored columns (4 specimens), and (iii) reference not drilled (as-built) columns (3 specimens). Compression tests have been carried out on extracted cores and, finally, on each column.

After the experimental campaign was concluded, the authors calibrated detailed finite element models based on the experimental results of the tests carried out on specimens. A software package able to fully account for the main nonlinear properties of concrete like, for instance, cracking and crushing, as well as the reduction of shear and compressive strength after cracking, has been used in setting up the finite element models made up of 3D tetrahedral elements [4]. The numerical models have been used to carefully evaluate the failure mode, especially for drilled specimens. This latter, indeed, are characterized by failure mechanisms different from as-built and restored specimens that causes their premature failure.

2 EXPERIMENTAL PROGRAM

In the framework of the experimental program carried out at the Laboratory of Structures of the University of Basilicata, totally 10 columns (out of 20 specimens available) have been subjected to compression test until failure. The program was intended to explore the effects of core drilling in RC members and the effectiveness of the holes' restoration. This latter, in comparison to the capacity of as-built specimens, not subjected to drilling nor restoration. For this reason, the specimens' range comprised as-built, drilled and drilled-restored columns, according to table 1. Restoration grout is an anti-shrinkage thixotropic mortar having compressive strength after one day equal to 30 MPa, and 50 MPa after 28 days.

Columns are 80 cm high with a cross-section of 30x30 cm with different longitudinal reinforcement. They were extracted from other specimens, namely full-scale beam-column joints tested in the same laboratory [7] during a previous experimental campaign. As can be seen in table 1, specimens are named "NS" or "S", depending on the beam-column joint they are extracted from, where S specimens are extracted from seismically designed joints and are provided of 8 mm diameter hoops (spaced 20 cm) and six 14mm diameter longitudinal bars. The only difference for NS specimens is that the number of longitudinal rebars is four instead of six.

This has no influence when computing confining effect according to confining models reported in the following, since the additional bars of S specimens are not restrained. Specimens show typical defects of real constructions, such as the variability of concrete cover thickness due to movements of the reinforcement during the casting operations.

Type	Column ID	f_c	Mean concrete cover
		MPa	mm
As-built	NS4	-	35.7
	NS7	-	37.5
	S4	-	45.0
Drilled	NS1	39.56	36.6
	S2	34.60	35.0
	S9	39.80	40.3
Drilled-restored	NS6	39.06	39.1
	S6	34.64	40.3
	S11	38.85	40.0
	S12	37.92	44.4

Table 1: List of 10 columns under investigation with concrete strength of extracted cores f_c, and detected concrete cover thickness.

In fact, table 1 reports also the concrete cover measured by means of the pacometer survey before testing. Only for drilled and drilled-restored columns, a concrete cylinder strength is shown. These values derive from the compression tests carried out on the extracted cores corrected through the method reported in [8]. This method allows taking into account drilling damage, shape factor of the core and possible presence of reinforcement inside the core specimen. Mean value of concrete strength reported in table 1 is f_{med}=37.88 MPa while the standard deviation is σ=2.09 MPa. Being the low value of the coefficient of variation CV=0.055, the mean value can be properly assumed as the concrete strength of as-built specimens.

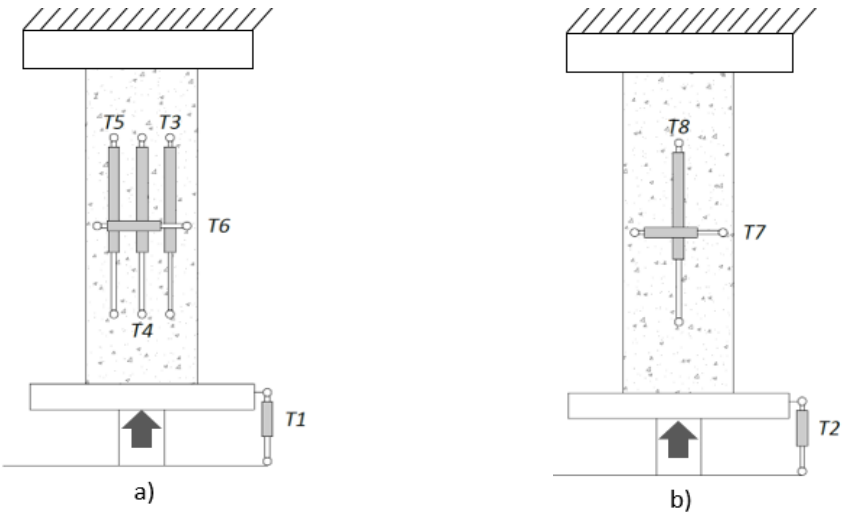

Figure 1: Loading schema and main instrumentation: a) on the front face and b) on the rear face.

The compression test machine applies the load moving his bottom plate and contrasting the top face of the specimen. The machine capacity is 3000 kN and the testing procedure is load controlled by applying increments of 30 kN/s until the peak load is found. When the load decreasing (after the peak is achieved) reaches 20% of the peak load, the machine unloads the specimen to start a new loading cycle. Figure 1 describes the loading scheme along with the instrumentation which consists of four Linear Variable Displacement Transducers (LVDT) placed on the front face of the specimens, one LVDT to measure the displacement of the bottom plate of the testing machine and additional 3 LVDT on the rear face. Out of these, two are placed on the concrete surface and one to measure the plate displacement on its opposite corner. Sometimes, an additional horizontal LVDT has been placed on the front face of the specimen like for example in fig. 2a). As examples, figure 2 shows the three types of tested columns placed on the Universal testing machine used throughout the experimental campaign. The front face is that where the core, if any, is drilled and possibly restored.

a) b) c)

Figure 2: a) as-built b) drilled and c) drilled-restored specimens before testing.

3 TEST RESULTS AND DISCUSSION

Different collapse mechanisms have been observed during the compression tests carried out on the three typologies of columns. Similar mechanisms have been found in as-built and drilled-restored in which a progressive deterioration of concrete cover is observed generally before reaching the peak load. The ultimate condition is, however, represented by the rebars' buckling which is poorly restrained due to the low amount of hoops. The drilled columns, as could be expected, are characterized by quite different behaviour especially in the first phases of compression tests. The first damage appears on the side of the hole in the front face, usually where the rebar is nearest to the hole. Figure 3 shows two stages of the compression test on S2 specimen. The first vertical crack appears on the left side of the hole (figure 3a) when the load is approaching the peak. In the following load cycles damage further concentrates in that region causing the buckling of the left bar (figure 3b). Uneven damage distribution causes eccentricity between load and resisting cross-section, which is an additional source of damage.

Results in terms of ultimate load measured on tested specimens are displayed in figure 4. The experimental ultimate load is averagely equal to 2293 kN for as-built specimens, 2260 kN for restored specimens and 1981 kN for drilled ones, respectively. So, drilled columns show a mean capacity reduction compared to as-built columns equal to about 14%. Restored columns show a reduction of only 1.4%, meaning that current procedures for restoring interventions

are effective. This conclusion has been drawn neglecting differences in terms of longitudinal reinforcement which can be considered small.

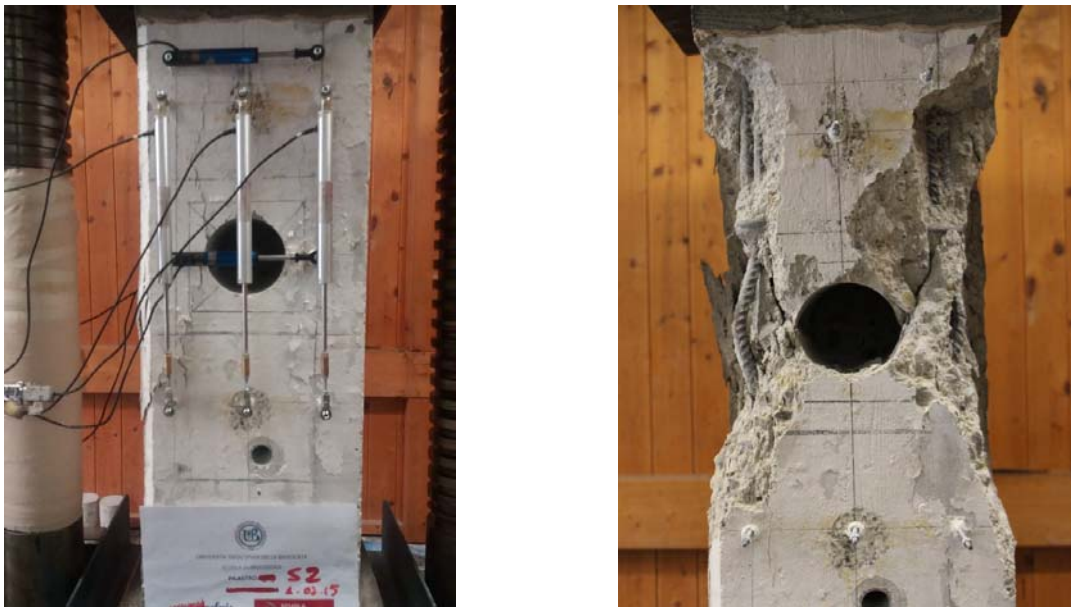

a) b)

Figure 3: S2 column: a) before peak load and b) at the end of the test.

Along with experimental results, also the analytical predictions of ultimate load for each column is reported. It is related to the gross concrete area times the compressive strength of each specimen added to the reinforcement contribution, as in expression (1):

$$F_{ug} = A_c \cdot f_c + A_s \cdot f_{ys} \tag{1}$$

where: A_c is the gross concrete area, A_s is the total steel area, f_{ys} is the steel yielding strength. For drilled specimens, A_c is obtained subtracting the horizontal projection of the hole which has 104 mm diameter and 220 mm depth.

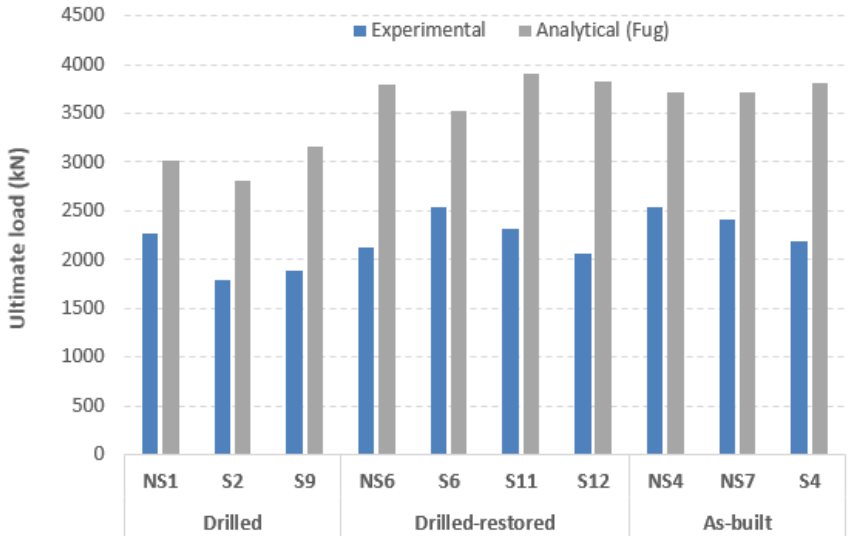

Figure 4: Comparison between experimental and analytical ultimate load values (gross section).

As can be seen, the analytical prediction of the ultimate load F_{ug} provides far higher values than the experimental ones. The observed scatter between experimental and analytical values is 52%, 67% and 58% for drilled, drilled-restored and as-built specimens, respectively. This difference strongly suggests that a much smaller value of the effective resisting cross section needs to be considered. This is also suggested by observing that in all tests concrete cover was spalled before reaching the peak load.

As a result, the effective section is assumed equal to the area confined by the steel cage, i.e. the gross section minus the concrete cover area (dashed area in figure 5). Moreover, in order to comply with international standards and codes for the design of concrete structures, the role of confining effect on concrete strength has been considered.

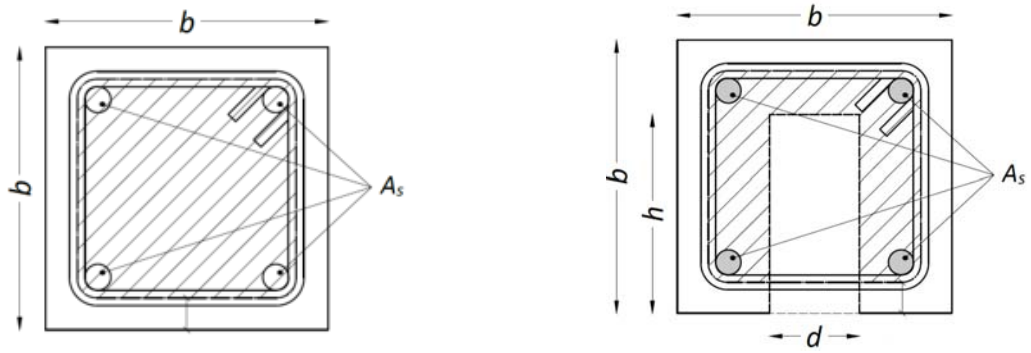

Figure 5: Effective cross section of a) as-built and drilled-restored and b) drilled specimens.

Some confinement models available in the literature [9,10] as well as the model reported in the Italian seismic code [1] have been considered. In the following, reference only to the model reported in [9] is made, because it provided the best matching with experimental results, while, for the sake of brevity, results obtained with the application of the other models are not discussed in the paper. By applying the confinement model in [9], a 5% increment of concrete strength is averagely obtained. Taking into account this concrete strength increase and the modified effective section displayed in figure 5, updated analytical values are computed and the comparison with the related experimental values is reported in figure 6.

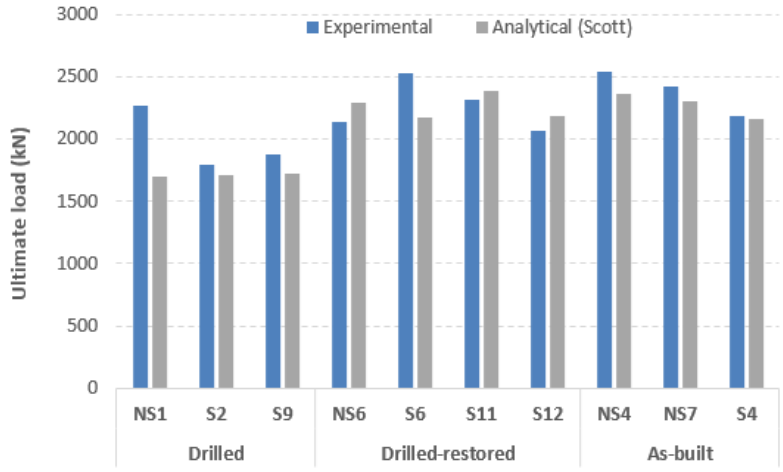

Figure 6: Comparison between experimental and analytical ultimate load values (confining model [9]).

As can be seen, the difference exp-num values remarkably decreases being averagely equal to 13%, 11% and 4% for drilled, drilled-restored and as-built specimens, respectively. Larger difference for drilled and drilled-restored specimens is somehow expected, due to the additional influence of the presence of the hole or the restoration unit on the collapse mechanism. Further, it is worth noting that, analytical results are always on the safe side for both as-built and drilled specimens, while, for drilled-restored specimens, they are generally higher thus unconservative.

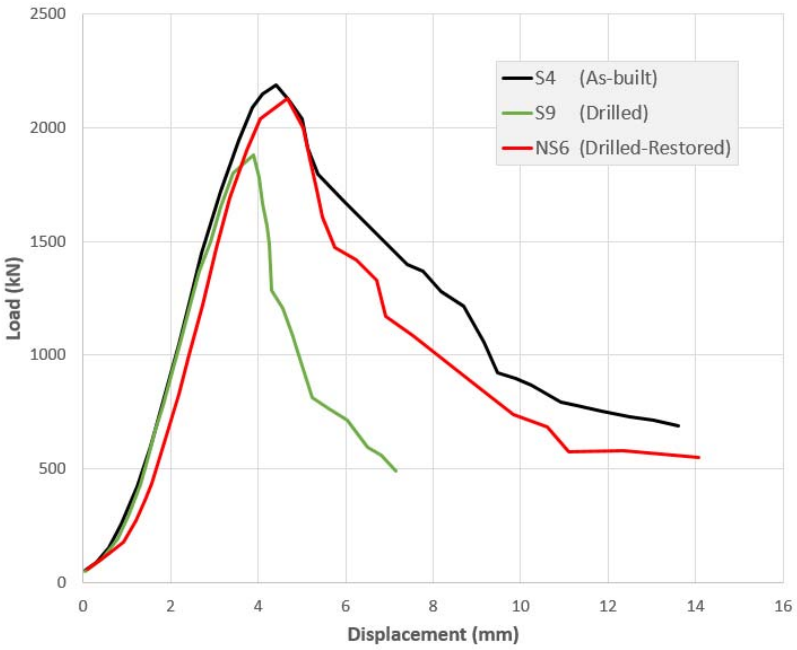

Figure 7: Envelope of skeleton curves of NS6, S4 and S9 specimens.

Although it seems inappropriate speaking of ductility for specimens whose failure is characterized by fragile mechanisms (concrete crushing and rebars' buckling), some differences have been found among the columns' typologies. In order to highlight this issue, the skeleton curves of the load-displacement envelopes have been plotted in figure 7 for three specimens: S4 (as-built), S9 (drilled) and NS6 (drilled-restored).

Beyond the expected lower failure load of the drilled column, degrading phenomena affecting as-built and drilled restored elements are more gradual. In fact, a 50% load reduction is found at displacements of 8 and 9 mm for drilled-restored and as-built specimens, respectively, while the drilled one shows the same reduction at around 5 mm. It is important to underline that restoration is able to provide the columns with almost the same ductile capacity compared with the as-built ones. Instead, more brittle failure is expected in drilled columns.

In addition to the previous discussion, it is worth remembering that specimens subject of this study belonged to seismically tested beam-column joints, whose concrete cover was mostly cracked at the moment of compression tests. Therefore, the reported results are particularly meaningful for seismically damaged structures for which residual capacity to carry vertical loads must be carefully evaluated, neglecting the contribution of the concrete cover.

4 FINITE ELEMENT ANALYSES

Nonlinear finite element models using ATENA 3D software package [4] were developed in order to more deeply investigate the failure mode found in drilled columns. The software is

based on the nonlinear fracture mechanics [11] and is capable to take into account compression softening as well as crushing and cracking of concrete.

For concrete, the robust smeared crack model "CC3DNonLinCementitious2" was used. The modelled column is NS1, that is a drilled one. The main properties of concrete are derived from the results of the compression test on the core extracted from the same column, that is f_c = 39.5MPa, f_t = 2.89 MPa, ν = 0.2, and E_c = 32.5 GPa, being respectively the compressive strength, tensile strength, Poisson ratio, and elastic modulus. Actually, with the exception of the compressive strength f_c, all other mechanical properties are derived from literature expressions based on f_c. As previously discussed, in accordance with the confinement model in [9], the concrete strength has been increased by 5%, assuming f_c=41.5 MPa in the numerical simulations.

A fictitious uniaxial stress-strain law (figure 8-a) with displacement based softening has been adopted [12].

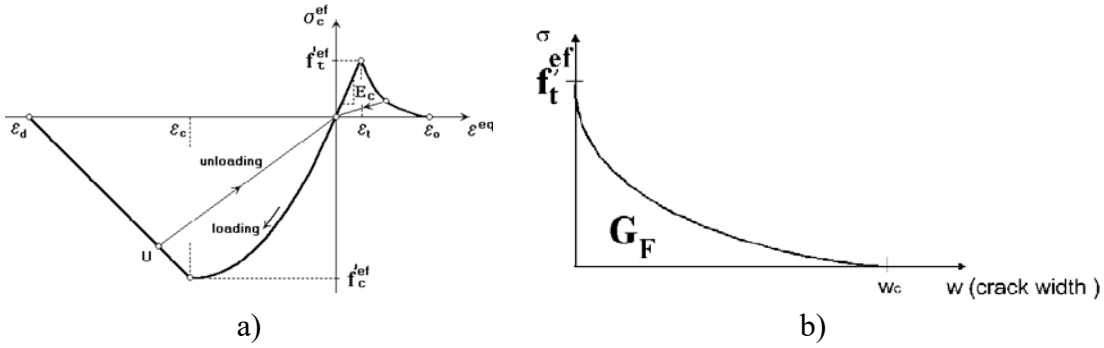

Figure 8: a) Uniaxial compressive stress-strain law and b) crack opening law for tensile stresses for concrete.

Under tensile stress, concrete behavior is governed by a crack opening law, as in figure 8-b defining the fracture energy (G_F). The tensile strength presents an exponential degrading law. The fracture energy was computed by means of Remmel's law [13].

An elastoplastic law with hardening was chosen for the reinforcing steel stress-strain relationship, with yielding strength f_y=480 MPa and failure strength f_t=590 MPa. These values were based on experimental tests carried out on rebars belonging to the same steel supply used for the specimens' construction. No bond slip between concrete and steel has been considered since the column is provided of ribbed bars and slip phenomena are not significant to global behavior under compression loads.

The global finite element model is referred to column NS1 without the concrete cover, based on the previous considerations, after having verified that the concrete cover is ineffective to increase the maximum load carrying capacity of the members under study. This means that only the concrete core inside the steel cage has been modeled giving a cross section 260mm x 260 mm.

Due to the presence of the core's hole, having diameter 104 mm and depth 220 mm, the mesh could not be structured (i.e. made of an ordinate repetition of elements having the same size). The mesh, in fact, is made of tetrahedral elements whose mean size near the hole is 10 mm while far from it, is set equal to 25 mm. The final mesh size has been determined by a sensitivity analysis gradually decreasing the element size. Despite only a short column is under study a huge model has been generated (figure 9-a). As a whole, the model is made up of 264 straight truss elements (i.e. carrying only axial loads) to simulate the steel reinforcement

(figure 9-b), 40347 tetrahedral elements to simulate concrete and the upper steel plate, and 9009 nodes. Analyzing such a model under cyclic loads is time expensive even using a powerful workstation, thus only monotonic analyses have been made to save time. Loading history was displacement controlled, applying to the top plate 5 mm displacement subdivided into 100 steps which the program can divide into further sub-steps based on numerical solution needs.

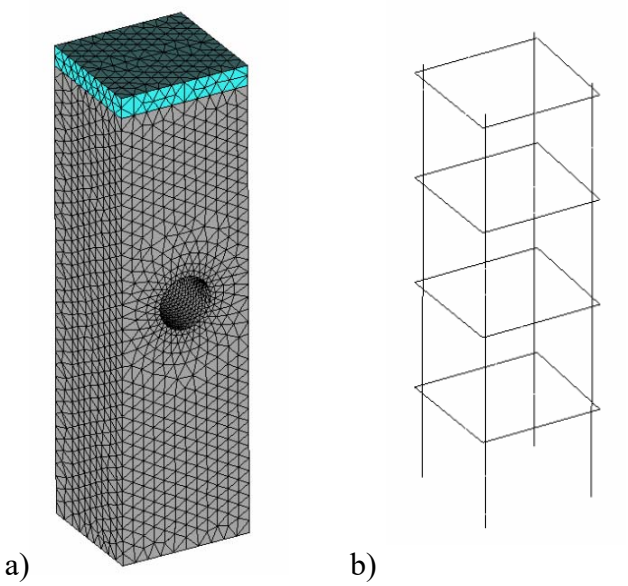

Figure 9: a) Mesh of NS1 FE model, b) steel reinforcement.

Firstly, to evaluate the effectiveness of the FEM model, experimental and numerical load-displacement curves are compared. As can be seen from figure 10, the peak load is well predicted by the numerical simulation, while differencence are found in the ascending branch, mainly ascribable due to the presence of a neoprene layer placed between the top face of column and the machine plate, having the role of uniformly applying the compression load during the test. Descending branches are not coincident due to the fact that numerical analysis is not cyclic and, then, generates less damage accompanied by a lower strength degradation.

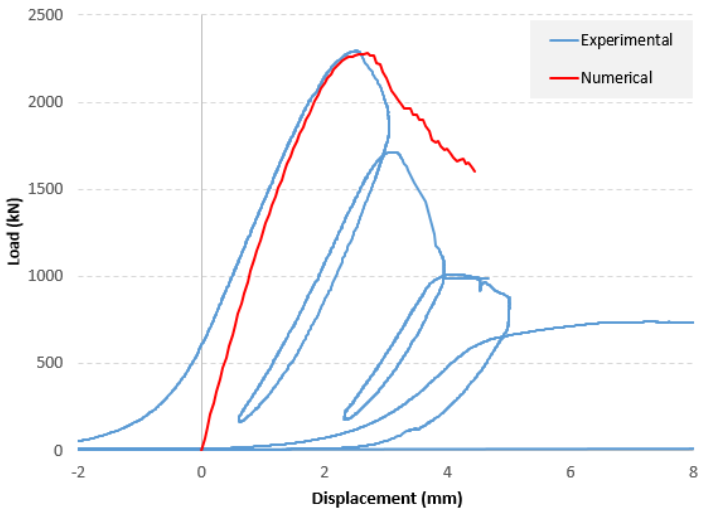

Figure 10: Experimental and numerical load-displacement curves for NS1 specimen.

4.1 Analysis of the failure mechanism

By studying the model of the drilled column NS1, the failure mode of the specimen due to presence of the extraction hole can be better understood. Specifically, figure 11a shows the deformed shape of the specimen by means of an isometric view and a side view. The presence of the hole determines an eccentricity between the applied load, directed along the column axis, and the center of the resisting section, not coincident with the column axis. This eccentricity introduces a bending moment around the X-axis with consequent displacements in the Y direction, especially for the column region around the hole.

Figure 11 shows the deformed shape at the peak load. Although horizontal displacements in the Y direction are low (below 1.0 mm), this involves an asymmetry of vertical (Z) displacements too.

This latter can be seen in figure 12a, where the relation between vertical displacements measured during the experimental tests by LVDT no. 4 (on the front face) and no. 8 (on the rear face) is displayed. As can be seen, there is a remarkable difference, matching the deformed shape obtained by the FEM model (figure 11).

Figures 12b and c display the colormap of Z displacements on the same faces of the specimen. From this colormap, similar differential displacements can be found between the points where the aforementioned LVDT are anchored.

This latter demonstrates the good calibration of the FEM model and its ability to predict the column's behavior.

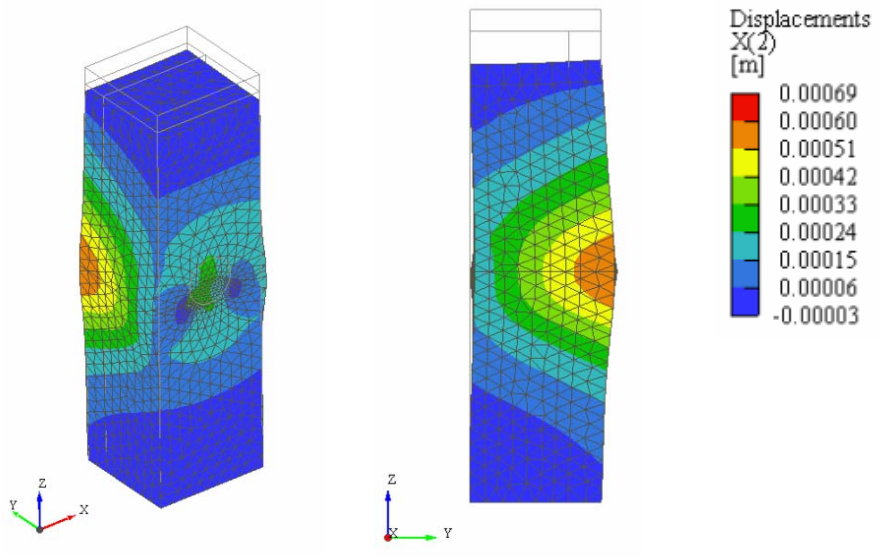

a) b)

Figure 11: Colormap of Y displacements as a) isometric view and b) side view.

In order to complete the description of the collapse mechanism, figure 13 shows the rebars' stresses at peak load. Longitudinal reinforcement (figure 13a) overcomes the yielding stress in compression (f_y=480 MPa), being the minimum value equal to 484 MPa. They are yielded for most of their length as can be seen by the evolution plotted along the bars' development. Going beyond the peak load of the specimen, the stress increases to about a maximum value of 500 MPa. This means that the bars do not fail being their tensile strength equal to 590 MPa.

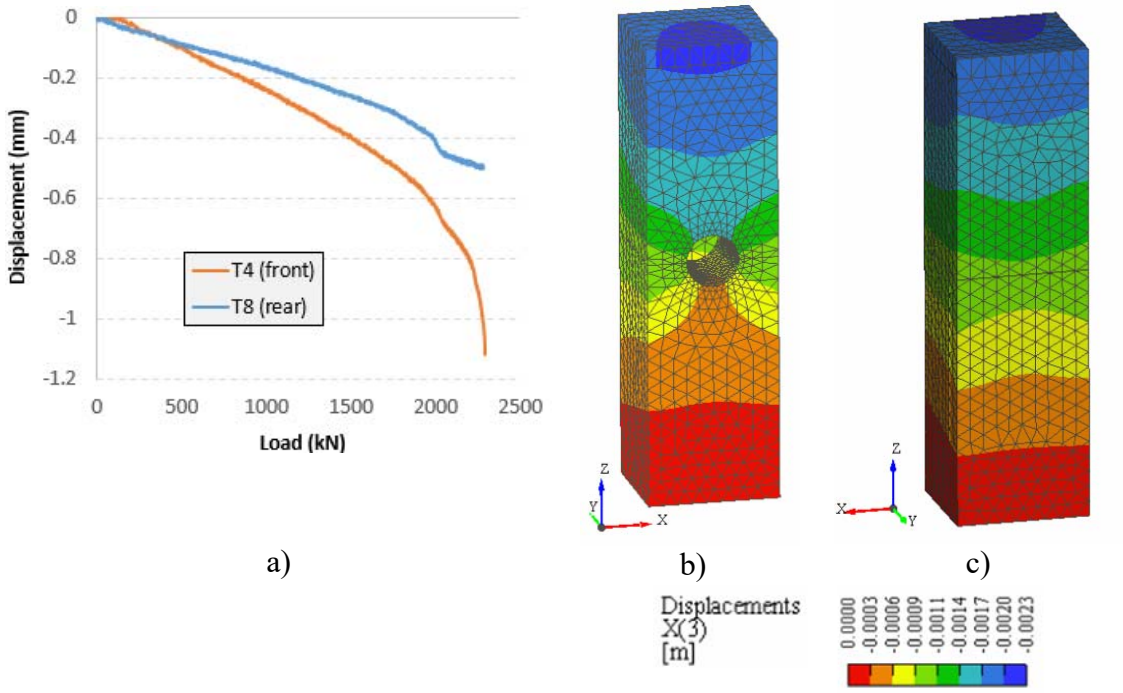

Figure 12: a) Experimental displacements and numerically evaluated on the front face (b) and on the rear face (c)

Hoops' stress is equal to 480 MPa corresponding to the yielding strength of steel. After the peak load, the hoops reach tensile stress values lower than 485 MPa. The most stressed branches of hoops are those normal to the core axis according to the deformed shape shown in figure 11a.

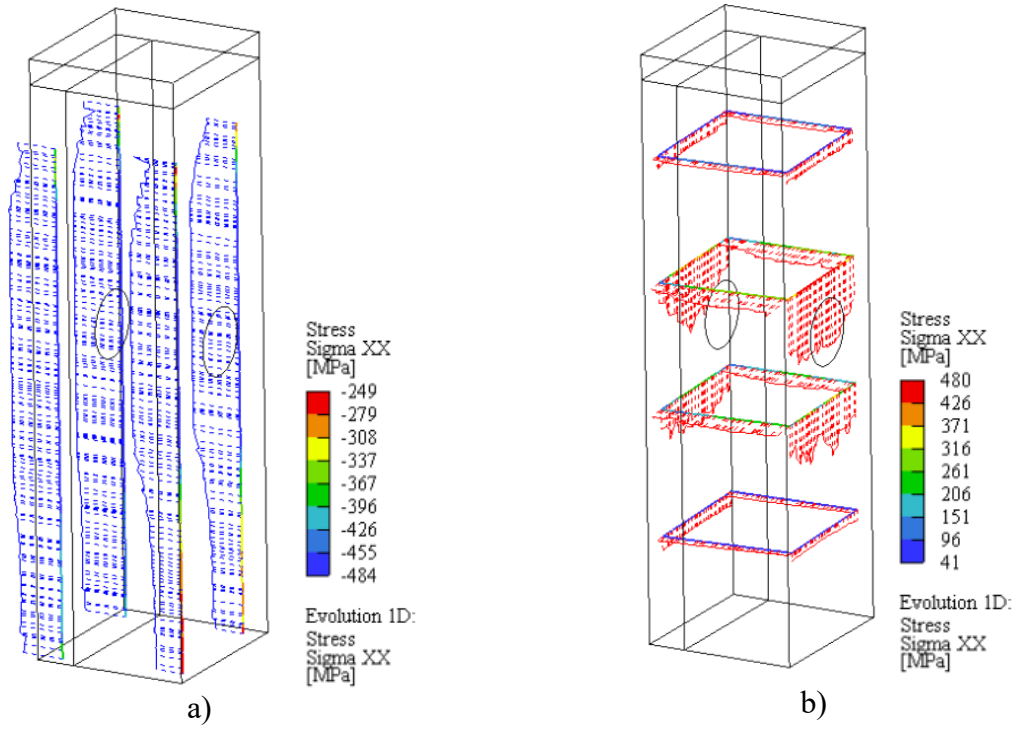

Figure 13: a) Longitudinal reinforcement and b) transverse reinforcement stresses distributions.

Summarizing, steel strength and ductility is not fully exploited as shown by the stress values achieved by longitudinal and transverse reinforcement. This happens because crushing of concrete on the core sides leads to the early buckling of reinforcement and consequent failure.

5 CONCLUSIONS

This paper reports a study on the behavior of reinforced concrete columns under axial compression load previously subjected to a seismic loading history as part of beam-column joints. By means of compression tests, the behavior of as-built, drilled and drilled-restored columns is investigated in order to evaluate the effect of core drilling and the effectiveness of the holes' restoration according to a standard procedure in the in-situ destructive testing campaign on RC buildings. Further, nonlinear finite element models were developed in order to better investigate the failure mode found in drilled columns.

The main findings from the experimental and numerical study are:

- Experimental results show that the failure of columns is characterized by early concrete cover spalling and consequent bar buckling. In particular, concrete cover spalling happens before reaching the peak load. Analytical ultimate load evaluated accounting for the gross concrete section is far higher than the correspondent experimental value.
- Based on the previous result, analytical prediction of the columns' strength can be done by considering only the confined concrete section, accounting also the confining effect. The most accurate capacity prediction is related to the confinement model reported in [9].
- Drilled specimens show a mean compression load capacity reduction equal to about 14% compared to as-built specimens. Restored specimens, instead, exhibit a negligible reduction (about 1.4%).
- Also, drilled specimens show a significant ductility reduction which has not been observed in restored specimens. This means that restoration is able to provide the columns with almost the same capacity of the as-built condition.
- The nonlinear FEM model of a drilled specimen showed a satisfying predictive capacity proved by the good agreement between experimental and numerical load-displacement curves.
- The failure behavior of columns is characterized by the eccentricity between the axial load and the resisting cross-section at the hole's location. This is clearly shown by the deformed shape of the numerical model that matches the experimental measurements of the LVDT placed on the front and rear face of the column.
- Finally, the failure of the studied column is characterized by the concrete crushing of regions around the hole. This causes the early spalling of concrete cover and consequent buckling of longitudinal bars that reach the compression yielding stress but are unable to exploit their full strength.

The experimental and numerical investigation on column specimens here reported suggests that the compression load carrying capacity of previously seismically loaded column members is far lower than that obtained from code-based analytical predictions accounting for the full cross-section. This is particularly true for weakly reinforced concrete columns as those of the present study, for which bar buckling can be not effectively restrained by hoops and ties.

ACKNOWLEDGEMENTS

The work reported in this paper was carried out within the framework of the DPC-ReLUIS 2018 Project, Research Line "Reinforced Concrete Structures", WP3-"Upgrading and Retrofitting of RC Existing Structures".

REFERENCES

[1] Aggiornamento delle *"Norme tecniche per le costruzioni"*, Ministry of Infrastructure DM 17 gennaio 2018, Suppl. ord. alla "Gazzetta Ufficiale n. 42 del 20 febbraio 2018 - Serie generale (in Italian), 2018.

[2] Masi A., Chiauzzi L. and Manfredi V., Criteria for identifying concrete homogeneous areas for the estimation of in-situ strength in RC buildings, *Construction and Building Materials*, **121**, 576-587, September 2016.

[3] Masi, A., Digrisolo, A., Santarsiero, G., Concrete strength variability in Italian RC buildings: Analysis of a large database of core tests. *Applied Mechanics and Materials,* ***5*97**, 283-290, 2014.

[4] Červenka V., Jendele L., Červenka J., *ATENA Program Documentation, Part 1, ATENA Theory Manual*. Cervenka Consulting, Praha, 2018.

[5] Z. P. Bažant, Q. Yu, Universal Size Effect Law and Effect of Crack Depth on Quasi-Brittle Structure Strength, *Journal of Engineering Mechanics,* **135**, 78-84, 2009.

[6] M. Brocca, Bažant Z.P., Size Effect in Concrete Columns: Finite-Element Analysis with Microplane Model, *Journal of Structural Engineering,* **127**(12), 1382-1390, 2001.

[7] Masi, A., Santarsiero, G., Nigro, D., Cyclic tests on external rc beam-column joints: Role of seismic design level and axial load value on the ultimate capacity. *Journal of Earthquake Engineering,* **1**7(1), 110-136, 2013.

[8] A. Masi, A. Digrisolo, and G. Santarsiero, Experimental Evaluation of Drilling Damage on the Strength of Cores Extracted from RC Buildings. *International Journal of Structural and Construction Engineering*, **7**, 2013.

[9] Scott, B.D., Park, R., and Priestley, M.J.N., *Stress-strain behavior of concrete confined by overlapping hoops at low and high strain rates*. J. American Concrete Institute, **79**, 13-27, 1982.

[10] J.B. Mander, M.J.N. Priestley, R. Park, Theoretical stress–strain model for confined concrete, *Journal of Structural Engineering*, ASCE **114** (8), 1804–1826, 1988.

[11] Z P. Bazant, *Fracture Mechanics Of Concrete Structures*, Elsevier Applied Science, London, 1992.

[12] Chen, W.F, Saleeb, A.F., *Constitutive Equations For Engineering Materials*, John Willey \& Sons, ISBN 0-471-09149-9, 1982.

[13] Remmel G., *Zum Zug-und Schubtragverhalten von Bauteilen aus Hochfestem Beton*. DAfStb, Heft 444, Beuth Verlag: Berlin, Germany, 1994.